

SPATIAL DISTRIBUTION OF STRONG GROUND MOTION CONSIDERING ASPERITY AND DIRECTIVITY OF FAULT

Shunroku YAMAMOTO¹

SUMMARY

Waveform simulations of the 1995 Hyogo-ken Nanbu earthquake were carried out to study effects of the fault parameters (*i.e.* radiation pattern, asperity, and directivity) on spatial distribution of strong ground motions around a near-field region. A fault model used in this study is proposed by Yoshida *et al.* [13] which has two prominent asperities, one is shallower and the other is deeper. The hypocenter is located between the two asperities. The computation code used here is after Hisada [2] which can compute a 3-D multi-layer Green's function efficiently. Calculation points are set radially around the epicenter (epicentral distances from 10 km – 90 km for 8 azimuths). Frequency range computed here is less than 1.42Hz. After simulations were done, we obtained the following results. 1) Overall attenuation relations (distance from the fault plane – peak horizontal velocity) almost agree with empirical values. However the largest amplitude does not always appear in the closest point to the fault plane especially in the near field. 2) Fault-normal motions have larger amplitude than fault-parallel motions in the near-field region. Radiation patterns of the asperities and directivity are most likely to play an important role to make the predominant component of motions. When an earthquake has a shallow strike-slip fault like this case, the above mentioned result is expected theoretically. 3) Calculation points effected by “forward directivity” from a shallower asperity show larger amplitude in this simulation. Since no strong motion seismograms were recorded around this area (near the Nojima fault) during the earthquake, we cannot confirm this result by real seismograms. However this simulation showed that location of asperities and characteristics of rupture on a fault drastically affect ground motion distribution in a near-field. 4) Duration of main phases is determined by both directivity and an asperity size. This combination sometimes makes a long-period pulse.

INTRODUCTION

Strong motion is generally known to be affected by combination of a source effect and a path effect. The both effects are usually difficult to treat in simulation, because a seismic source and an underground structure are not always simple enough to model easily, further more, we do not have much information on them. The 1995 Hyogo-ken Nanbu earthquake ($M_{JMA}=7.2$) is one of rare cases of which we can have dynamic source models and underground velocity structures as well as near-field strong motion records.

Just after the earthquake, Kikuchi[8] showed far-field waveforms are well explained by superposition of three different point sources. This indicates that the event is a multiple shock or has three large asperities. After amount of recorded data were compiled, slip distributions of the fault plane were proposed by many researchers. Wald [12] carried out a waveform inversion of the slip history using near-field and far-field waveforms together. Hashimoto *et al.* [1] searched for sets of displacement of the fault model by using GPS data. Yoshida *et al.* [13] computed a joint inversion using geodetic data, near-field waveforms, and far-field waveforms. Horikawa *et al.* [3] also used an inversion scheme by geodetic and strong motion data to obtained a slip history of the earthquake. Sekiguchi *et al.* [10] determined location of asperities precisely by checking the particle motion of near-field records. Ide *et al.*[4] performed an inversion using strong motion data near the epicenter. Most of

¹ National Research Inst for Earth Science and Disaster Prevention, Japan, Email: syama@geo.bosai.go.jp

those studies assumed the earthquake consists of two fault planes, one plane (the Nojima fault) is located beneath Awaji Island, and the other (the Kobe fault system) beneath the Kobe area. They generally resulted that the rupture started at the deepest point between the two planes (beneath Akashi Strait). As the rupture propagated, the first large asperity ruptured in a deeper west part of the Suma fault (one of the Kobe fault system), then another large asperity ruptured in a shallower part of the Nojima fault. In some studies another small asperity can be seen in the middle of the Kobe fault system. Some studies indicate the prominent phases, which dominate less than 1 Hz, observed around the Kobe area during the earthquake are mainly caused by those asperities (i.e. Sekiguchi *et al.* [10]).

On the other hand, several studies (i.e. Kikuchi [9]) reported that the largest phase, near the source region, is predominant in the fault-normal direction. It is a typical effect caused by combination of a radiation pattern and directivity of a rupture propagation (Somerville and Graves [11]) in the case of strike slips. If a rupture is unilateral and slip distribution is homogeneous, this effect is the easiest to explain. However, if asperities are introduced to a source model, the problem becomes to be more complex and more realistic. In this sense, to investigate an effect caused by combination of asperities and directivity seems to be very important. Herein waveform simulations of the 1995 Hyogo-ken Nanbu earthquake are carried out to study mainly a realistic effect of asperities and directivity of the fault.

SOURCE AND VELOCITY MODEL

Several fault models are proposed for the 1995 Hyogo-ken Nanbu earthquake as mentioned above. The fault model proposed by Yoshida *et al.* [13] is chosen in this study, because this model is derived from larger number of near-field strong motion data, far-field data as well as geodetic data and simulates near-field ground motions relatively well. The model consists of two fault planes, one is the Nojima fault and the other the Kobe fault system (originally the Suma/Suwayama/Gosukebashi fault). In the model, the Nojima fault and the Kobe fault system are divided by 6*4 and 9*4 subfaults respectively. A source time function of each subfault is superposed by three ramp functions with 1.0 sec interval. Main source parameters are shown in Table 1 and overall slip distribution is shown in Figure 1. As shown in Figure 1, this event is roughly a right-lateral strike slip. By checking Figure 1 in detail, it is understood one large asperity is located in the bottom of the Kobe fault system, and another one in a shallower part of the Nojima fault. Locations and sizes of those two asperities seem to be clue to explain long-period pulses recorded around the Kobe region.

As for a deeper velocity structure, the four-layer model by Yoshida *et al.* [13] is used. The shallowest layer of this model has S-wave velocity of 3200 m/sec and the thickness is 2.0 km and the deepest one has S-wave velocity of 4500 m/sec. In this study, a three-layer subsurface structure is introduced into the original structure model in order to simulate amplitude of higher frequencies. a subsurface model is selected according to the subsurface model proposed by Iwata *et al.* [6]. The uppermost layer has S-wave velocity of 550 m/sec and the thickness is 0.16 km. Many studies indicate existence of a clear edge of the bedrock near Rokko Mountains. For example, Kawase and Hayashi [7] demonstrated that the edge is one of the main reasons to give serious damage to a certain part of Kobe City. Though a real subsurface structure is irregular and inhomogeneous, 1-D heterogeneity is assumed in this study to avoid complex influence of local site responses. A 1-D seven-layer velocity model used here is shown in Table 2.

SIMULATION METHOD

The computation code is based on a method of Hisada [2] which can compute a multi-layer Green's function efficiently by using analytical asymptotic solutions. In this study, sets of solutions for 3-D multi-layer Green's functions between a source and a receiver point are computed first. Those sets are stored in a memory as a Green's function library. Second, waveforms at each calculation point are integrated by using the best sets a Green's function library. It is very efficient to compute a problem with a complex slip history, because calculations of Green's functions, which are time consuming, are done only once independent of complexity of a slip history.

In order to investigate spatial change of seismic waves (waveform and amplitude), calculation points are put radially on a surface around the epicenter. Each point has epicentral distance of 10, 20, 30, 50, 70, and 90 km for 8 different azimuths (i.e. N0E, N45E, N90E, N135E, N180E, N225E, N270E, and N315E). Frequency range calculated here is less than 1.42 Hz. Location of the faults and calculation points is shown in Figure 2.

RESULTS AND DISCUSSION

Simulations by the original source model by Yoshida *et al.* [13] with a seven-layer velocity structure are computed in this study, and velocities at each calculation point and attenuation relations are obtained.

Calculated velocities

First, velocities computed at each calculation point are shown in Figure 3 (a), (b), (c). Roughly, velocities of NS component and EW component have similar amplitude at each point. If we look at velocities of 10 – 30 km points on the N45E and N225E lines, which are located almost parallel to the faults, peak velocities appear at the same time for NS and EW components and polarities of both components are opposite. This indicates that a fault-normal component is dominant for these points. These phases look like long-period pulses whose duration are 2 – 3 sec for the N45E line and 2 – 5 sec for the N225E line. By checking travel-time and sizes of asperities, velocities at the N45E line seem to be influenced by the asperity of the Kobe fault system and velocities at the N225E line are influenced by the asperity of the Nojima fault. Though both asperities have almost same dislocation and sizes, velocities at the N225E line have larger amplitude and longer duration, because the calculation points are located much closer to the asperity and effected largely by forward directivity, further, propagation distance of the rupture is longer in this case. As we do not have observation records nearby the Nojima fault, comparison cannot be done with real data unfortunately. Velocities at the N135E and N315E lines show another interesting feature. They look like a rather simple shape; their main phases are predominant in fault-parallel component and have longer duration because two pulses from the different asperities are superposed at these points. Since the waveforms are effected by backward directivity, amplitude is smaller and duration becomes longer.

In general, calculated velocities show some complexity in the near-field region, however, in the far-field, characteristics of velocities become to be homogenised. In most of the case, main phases are almost explained by characteristics of asperities and a rupture process in the near field. To know a radiation pattern and a size of the closest asperity, as well as a rupture process is very important when we try to understand a feature of strong ground motions.

Attenuation relation

Second, an attenuation relation (epicentral distance – calculated peak horizontal velocity) is shown in Figure 4. Though epicentral distances sometimes used as a parameter to estimate peak ground motions, this figure indicates variation of the estimated values is very large for an entire distance. This is the simplest method, but has a large error too. Figure 5 shows another attenuation relation (distance from the fault plane – calculated peak horizontal velocity) accompanied with empirical values (Irikura and Fukushima [5]). The empirical values are estimated by assuming that surface is a rock ($V_s=700$ m/sec). According to Figure 5, calculated values are generally smaller than the empirical values but its shape is similar to empirical values. While variation is more stable than the case of Figure 4, the calculated values still vary widely in the near-field region and it is clear that amplitude at the closest point to the fault is not always to be the largest. This is caused by inhomogeneous distribution of slip on the fault planes (*i.e.* location of asperities) and a directivity effect. This indicates locations and sizes of asperities, as well as directivity, are very important when one simulates near-field strong motions.

Figure 6 shows comparison of attenuation relations between peak horizontal velocities and peak vertical velocities. It is well known by observation data that a vertical component is usually smaller than a horizontal component. The calculated results support this. As we look at Figure 6 in detail, peak values of a vertical component are not stable even in the far-field region comparing with horizontal values. A vertical component seems to be effected by source characteristics more sensitively.

CONCLUSIONS

Simulations of the 1995 Hyogo-ken Nanbu earthquake ($M_{JMA}=7.2$) are carried out, and the following results are obtained. 1) Attenuation relations (distance from the fault plane – peak horizontal velocity) almost agree with empirical values. However the largest amplitude does not always appear in the closest point to the epicenter. 2) Main phases are predominant in fault-normal components. A radiation pattern of the asperities and directivity are likely to play an important role to make the predominant component of motions. When an earthquake has a shallow strike-slip fault like this case, the above mentioned result is expected theoretically. 3) Velocities at the points effected by forward directivity from a shallower asperity show larger amplitude. Since no strong motion seismograms were recorded around this area (the Awaji area) during the earthquake, we cannot confirm this

result by real recorded data. However this simulation showed that distribution of asperities and characteristics of a rupture on a fault drastically affect ground motion distribution in a near-field region. 4) Duration of main phases is determined by both directivity and sizes of asperities. This combination sometimes makes long-period pulses like recorded data around Kobe City.

ACKNOWLEDGEMENT

The digital data of the source model were provided by K. Koketsu. Discussion with Y. Hisada, H. Kawase, and S. Matsushima was very fruitful.

REFERENCES

1. Hashimoto, M., Sagiya, T., Tsuji, H., Hatanaka, Y., and Tada, T. (1996), "Co-seismic displacements of the 1995 Hyogo-ken nanbu earthquake", *J. Phys. Earth*, 44, pp255-279.
2. Hisada, Y. (1995), "An efficient method for computing green's functions for a layered half-space with sources and receivers at close depths (Part2)", *Bull. Seism. Soc. Am.*, 85, pp1080-1093.
3. Horikawa, H., Hirahara, K., Umeda, Y., Hashimoto, M., and Kusano, F. (1996), "Simultaneous inversion of geodetic and strong motion data for the source process of the Hyogo-ken Nanbu, Japan, earthquake", *J. Phys. Earth*, 44, pp455-471.
4. Ide, S., Takeo, M., and Yoshida, Y. (1996), "Source process of the 1995 Kobe earthquake: determination of spatio-temporal slip distribution by Bayesian modeling", *Bull. Seism. Soc. Am.*, 86, pp547-566.
5. Irikura, K. and Fukushima, Y. (1995), "Attenuation characteristics of peak amplitude in the Hyogoken Nanbu earthquake", *Report of the Grant-In-Aid for Science Research*, No.05302069, pp11-18.
6. Iwata, T., Hatayama K., Kawase H., and Irikura K. (1996), "Site amplification of ground motions during aftershocks of the 1995 Hyogo-ken Nanbu earthquake in severely damaged zone – array observation of ground motions in Higahinada ward, Kobe City, Japan –", *J. Phys. Earth*, 44, pp553-561.
7. Kawase, H. and Hayashi, Y. (1996), "Strong motion simulation in Chuo ward, Kobe, during the Hyogo-ken Nanbu earthquake of 1995 based on the inverted bedrock motion", *J. Struct. Contr. Eng., AIJ*, 480, pp67-76 (in Japanese).
8. Kikuchi, M. (1995), "Source mechanism by teleseismic body-waves", *Chikyuu*, No.13, pp47-53 (in Japanese).
9. Kikuchi, M. (1995), "A shopping trolley seismograph", *Nature*, 377, p19.
10. Sekiguchi, H., Irikura, K., Iwata, T., Kakehi, Y., and Hoshiya, M. (1996), "Minute location of faulting beneath Kobe and the waveform inversion of the source process during the 1995 Hyogo-ken Nanbu, Japan, earthquake using strong ground motion records", *J. Phys. Earth*, 44, pp473-487.
11. Somerville, P. and Graves, R. (1993), "Conditions that gives rise to unusually large long period ground motions", *The Structural Design of Tall Buildings*, 2, pp211-231.
12. Wald, D.J. (1995), "A preliminary dislocation model for the 1995 Kobe (Hyogo-ken nanbu), japan, earthquake determined from strong motion and teleseismic waveforms", *Seism. Res. Lett.*, 66, pp22-28.
13. Yoshida, S., Koketsu, K., Shibazaki, B., Kato, T., and Yoshida, Y. (1996), "Joint inversion of near- and far-field waveforms and geodetic data for the rupture process of the 1995 Kobe earthquake", *J. Phys. Earth*, 44, pp437-454.

Table 1: Source parameters (after Yoshida *et al.* [13])

paramter	Nojima fault	Suma/Suwayama/Gosukebashi fault
Strike (degree)	N43E	N232E
Dip (degree)	75	85
Length (m)	24000	36000
Width (m)	16000	16000
Depth of upper edge (m)	5	100
Number of subfaults	6*4	9*4

Table 2: Velocity structure used in this study

Density (g/cm ³)	Vp (m/sec)	Qp	Vs (m/sec)	Qs	Thickness (m)
2.00	1800.0	300.0	550.0	70.0	160.0
2.20	2500.0	300.0	1000.0	100.0	240.0
2.30	4250.0	300.0	2850.0	150.0	400.0
2.60	5500.0	300.0	3200.0	150.0	2000.0
2.70	6000.0	500.0	3460.0	250.0	20000.0
2.80	6600.0	800.0	3810.0	400.0	10000.0
3.00	7800.0	1000.0	4500.0	500.0	--

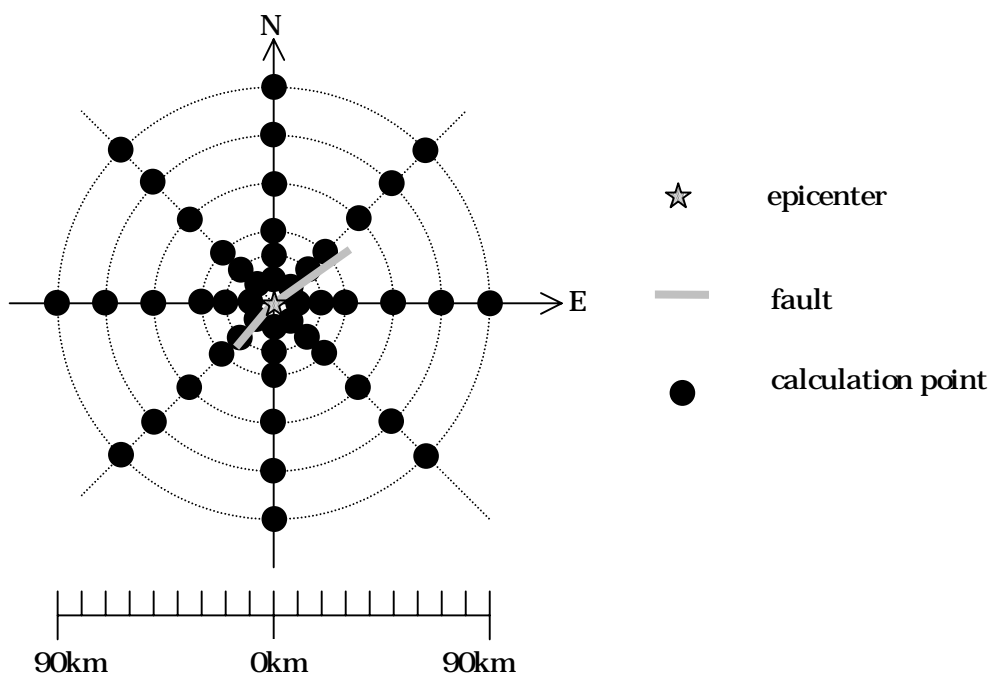


Figure 1: Locations of the faults and calculation points

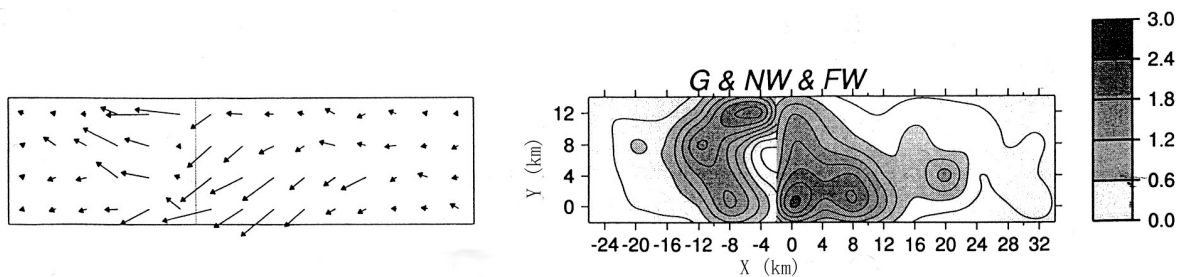
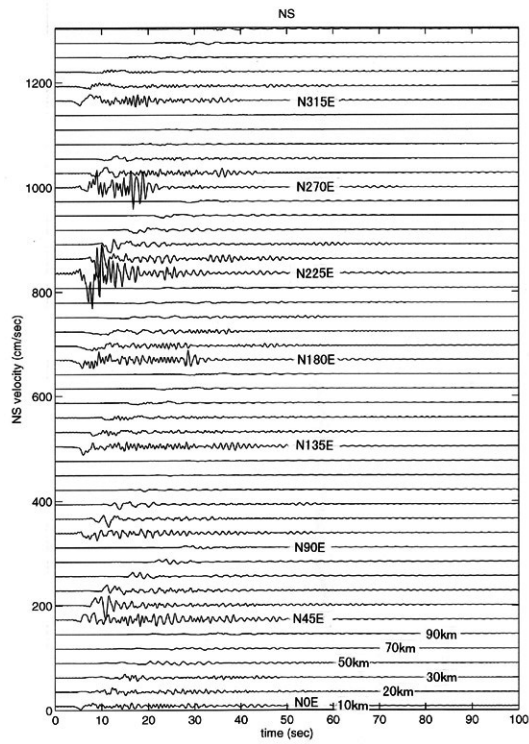
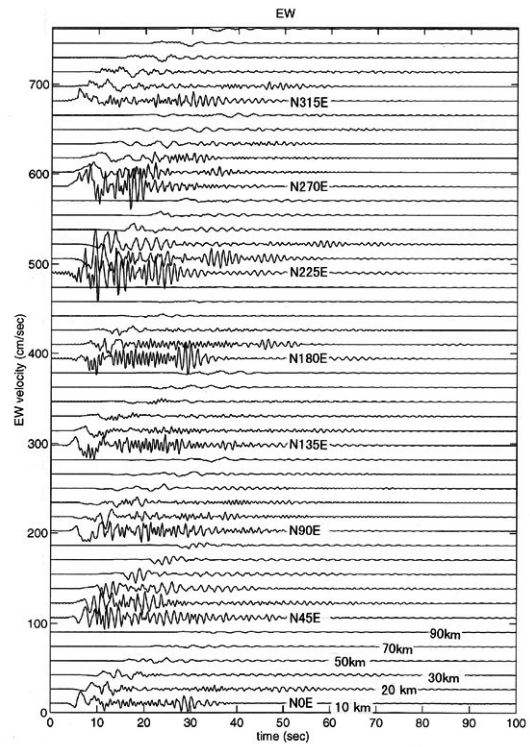


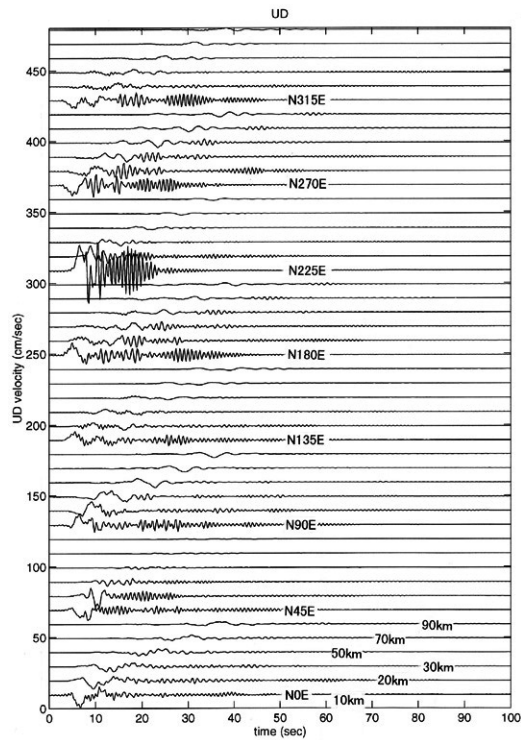
Figure 2: Slip distribution of the source model (Yoshida *et al.* [13])



(a) NS component



(b) EW component



(c) UD component

Figure 3: Calculated velocities

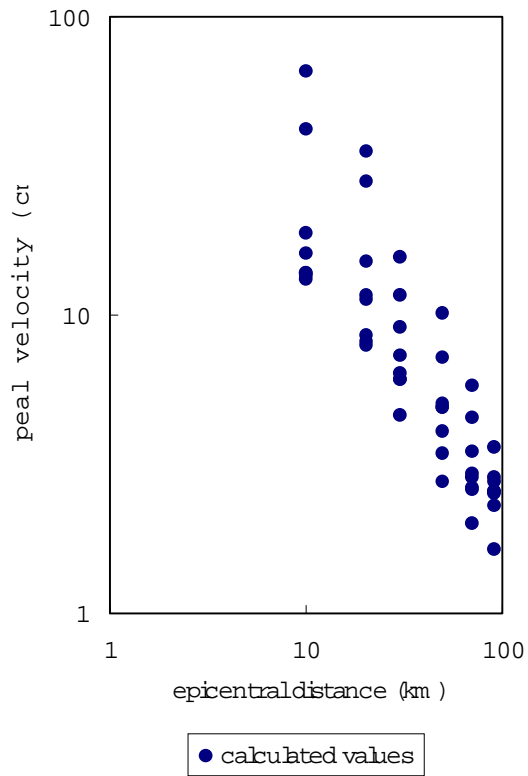


Figure 4: Attenuation relation

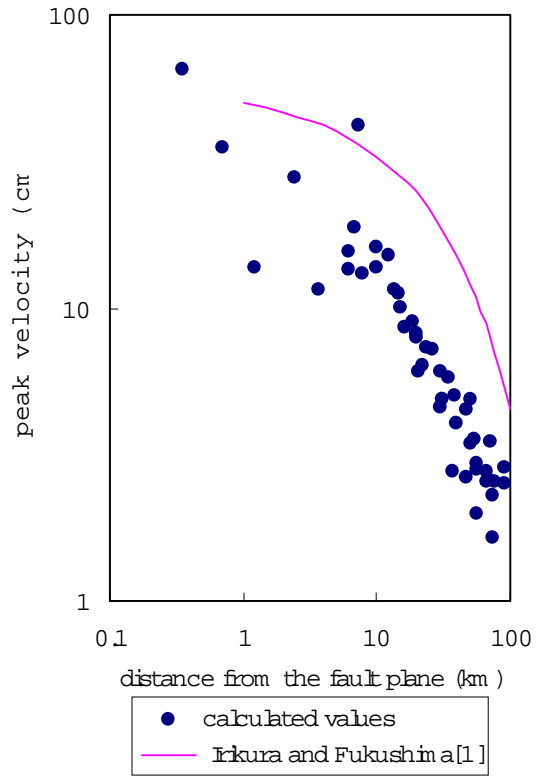


Figure 5: Attenuation relation

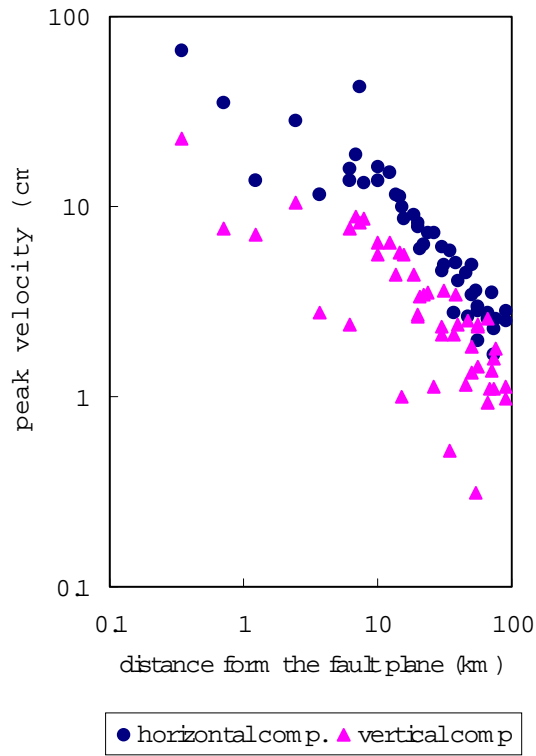


Figure 6: Attenuation relation